The ND5 Subunit Was Labeled by a Photoaffinity Analogue of Fenpyroximate in Bovine Mitochondrial Complex I†

Eiko Nakamaru-Ogiso,‡ Kimitoshi Sakamoto,§ Akemi Matsuno-Yagi,‡ Hideto Miyoshi,§ and Takao Yagi*,‡

Division of Biochemistry, Department of Molecular and Experimental Medicine, The Scripps Research Institute, La Jolla, California 92037, and Division of Applied Life Sciences, Graduate School of Agriculture, Kyoto University, Kyoto 606-8502, Japan

Received October 8, 2002; Revised Manuscript Received December 2, 2002

ABSTRACT: Fenpyroximate is a potent inhibitor of the mitochondrial proton-translocating NADH−quinone oxidoreductase (complex I). We synthesized its photoaffinity analogue [^{3}H](trifluoromethyl)phenyldiazirinylfenpyroximate ([^{3}H]TDF). When bovine heart submitochondrial particles (SMP) were illuminated with UV light in the presence of [^{3}H]TDF, radioactivity was mostly incorporated into a 50 kDa band. There was a good correlation between radioactivity labeling of the 50 kDa band and inhibition of the NADH oxidase activity, indicating that a 50 kDa protein is responsible for the inactivation of complex I. Blue native gel electrophoresis of the [^{3}H]TDF-labeled SMP revealed that the majority of radioactivity was found in complex I. Analysis of the complex I band on an SDS gel showed a major peak of radioactivity at ∼50 kDa. There are three subunits in complex I that migrate in this region: FP51K, IP49K, and ND5. Further analysis using the 2D gel electrophoresis implied that the labeled protein was the ND5 subunit. Labeling of the ND5 subunit was stimulated by NADH/NADPH but was prevented by various complex I inhibitors. Amiloride derivatives that are known to be inhibitors of Na^+/H^+ antiporters also diminished the labeling. In agreement with the protective effect, we observed that the amiloride derivatives inhibited NADH−ubiquinone-1 reductase activity but not NADH−$K_3Fe(CN)_6$ reductase activity in bovine SMP. These results suggest that the ND5 subunit is involved in construction of the inhibitor- and quinone-binding site(s). Furthermore, it seems likely that the ND5 subunit may participate in $H^+(Na^+)$ translocation in coupling site 1.

Oxidative phosphorylation is a fundamental, universal process in mammalian cells to generate the energy source ATP (*1*, *2*). During this process, a series of membrane-bound multiprotein complexes translocate protons across the membrane, coupled with redox reaction. Mitochondrial proton-translocating NADH−quinone oxidoreductase (complex I;[1] EC 1.6.99.3) is located in the entry of this process and recognized as one of the largest and the most complicated membrane-associated enzyme complexes with a total mass close to 1000 kDa (*3*). It consists of at least 43 different subunits (*4*), seven of which are encoded by mitochondrial DNA (designated ND1−6 and 4L) (*5*, *6*) and the others by nuclear DNA (*7*). Since structural and functional defects of complex I are reported to be a primary cause in many cases of mitochondrial diseases, studies of complex I have been of growing interest in the wide range of life science fields (*8*, *9*).

Despite recent remarkable progress in complex I research (*10*), our knowledge about the electron-transport pathway, proton translocation mechanism, and mode of action of numerous specific inhibitors that are thought to compete for the quinone- (Q-) binding site(s), are still largely limited. The structure−activity relationships developed by using inhibitors have provided important insights into the functional architecture of this complicated enzyme system (*11*, *12*). Earlier studies with two rotenone-derived photoaffinity probes located a single inhibitor-binding site in the ND1 subunit (*13*, *14*). Also, [^{14}C]-*N*,*N*′-dicyclohexylcarbodiimide, a classical carboxyl group modifying reagent, was shown to label the ND1 subunit (*15*−*17*). In *Neurospora crassa*, a photoreactive UQ analogue specifically labeled the 9.5 kDa subunit (homologue of the B9 subunit in bovine enzyme), which was replaced by UQ2 but not by rotenone (*18*, *19*). A recent study with a photoaffinity analogue of pyridaben, an inhibitor more potent than rotenone, showed that the PSST subunit contained the inhibitor-binding site (*20*). The PSST subunit was proposed to house iron−sulfur cluster N2, which has the highest redox potential and is therefore considered to be the site of electron transfer to the Q molecules (*21*).

† This work was supported by U.S. Public Health Service Grant R01GM33712. This is Publication 15258-MEM from The Scripps Research Institute, La Jolla, CA.

* To whom correspondence should be addressed. E-mail: yagi@scripps.edu.

‡ The Scripps Research Institute.

§ Kyoto University.

[1] Abbreviations: complex I, mitochondrial proton-translocating NADH−quinone oxidoreductase; [^{3}H]TDF, [^{3}H](trifluoromethyl)phenyldiazirinylfenpyroximate; Q, quinone; UQ, ubiquinone; SMP, submitochondrial particles; UQ1, ubiquinone-1; EIPA, 5-(*N*-ethyl-*N*-isopropyl)amiloride; MIA, 5-(*N*-methyl-*N*-isobutyl)amiloride; SDS−PAGE, sodium dodecyl sulfate−polyacrylamide gel electrophoresis; BN-PAGE, blue native gel electrophoresis; 2-DE, two-dimensional electrophoresis; IEF, isoelectric focusing; CBB, Coomassie Brilliant Blue; PVDF, poly(vinylidene difluoride); NDH-1, bacterial proton-translocating NADH−quinone oxidoreductase; FP, flavin protein subcomplex of bovine complex I; IP, iron−sulfur protein subcomplex of bovine complex I; BSA, bovine serum albumin; EM, electron microscopy.

10.1021/bi0269660 CCC: $25.00
Published on Web 12/31/2002

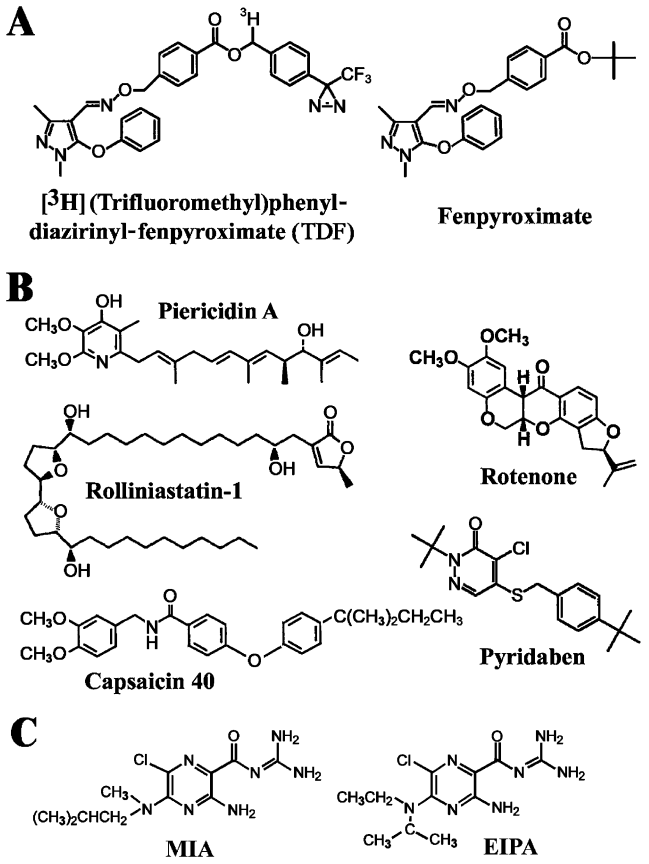

FIGURE 1: Structures of the photoaffinity probe [^{3}H](trifluoromethyl)phenyldiazirinylfenpyroximate ([^{3}H]TDF) and its prototype fenpyroximate (A), other complex I inhibitors (B), and Na^+/H^+ antiport inhibitors and amiloride derivatives (C) used in this study.

Site-directed mutation experiments suggest that the NuoD subunit (Nqo4/IP 49 kDa homologue) is involved in rotenone/piericidin A binding (*22*−*24*). A recent paper on cross-linking experiments and heterologous expression indicated that the Nqo7 subunit (ND3/NuoA homologue) directly interacts with the Nqo6 subunit (PSST/NuoB homologue) and provides a membrane foundation for the Nqo6 subunit in the *Paracoccus denitrificans* NDH-1 (*25*). Therefore, the subunits IP 49 kDa, PSST, ND1, and ND3 are believed to construct an inhibitor-binding pocket(s) in complex I/NDH-1 (*24*, *26*). Fenpyroximate has been established to be a potent inhibitor of complex I/NDH-1 (*11*, *27*). However, it is significantly different from pyridaben structurally (Figure 1). It was, therefore, anticipated that fenpyroximate might provide additional, but unique, insight into the inhibitor-binding sites in complex I.

In this study, we synthesized a photaffinity analogue of fenpyroximate [[^{3}H](trifluoromethyl)phenyldiazirinylfenpyroximate ([^{3}H]TDF)] as shown in Figure 1A and carried out identification and characterization of the labeled subunits in bovine heart complex I.

MATERIALS AND METHODS

Materials. Bovine heart mitochondria were generously provided by Dr. C.-A. Yu (Oklahoma State University). SMP were prepared as described in ref *28*. Rolliniastatin I was a gift from Dr. E. Estornell (University of Valencia); piericidin A was from Dr. S. Yoshida (Riken, Japan). 5-(*N*-Ethyl-*N*-isopropyl)amiloride (EIPA) and 5-(*N*-methyl-*N*-isobutyl)-amiloride (MIA) were from Sigma. Monoclonal mouse anti-39 kDa antibody was from Molecular Probes (Eugene, OR). Antisera against the bovine IP 49 kDa and FP 51 kDa subunits were kindly provided by Dr. Y. Hatefi (The Scripps Research Institute).

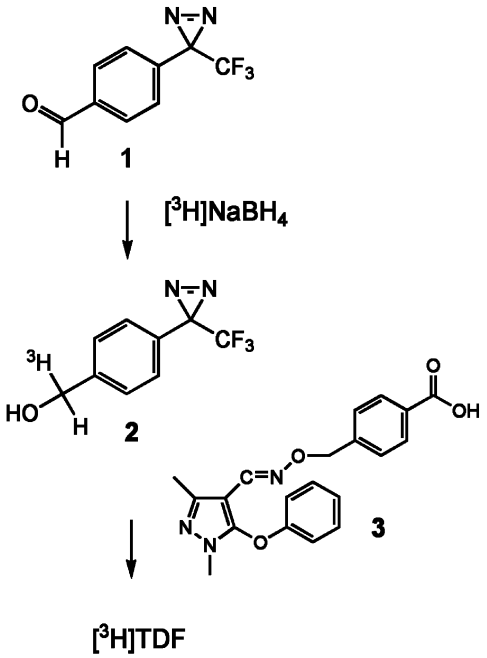

FIGURE 2: Synthesis of [^{3}H]TDF. See Materials and Methods for details.

Synthetic Procedures of [^{3}H]TDF. The synthetic scheme of [^{3}H](trifluoromethyl)phenyldiazirinylfenpyroximate ([^{3}H]-TDF) is shown in Figure 2. The benzaldehyde (compound **1**) was prepared by the method of Resek et al. (*29*). The aldehyde (compound **1**) (7.5 mg, 35 μmol) was reduced with [^{3}H]$NaBH_4$ (500 mCi/18.5 GBq, 85 Ci/mmol, 5.88 μmol) from American Radiolabeled Chemicals (St. Louis, MO) dissolved in 75 μL of 0.01 M NaOH to afford the alcohol (compound **2**). To chilled 2-propanol solution containing the acid (compound **3**) (13 mg, 35.6 μmol), which was a kind gift from Nihon Nohyaku Co., Ltd., was added the above reaction mixture in the presence of 1-(3-dimethylaminopropyl)-3-ethylcarbodiimide (27 mg, 140 μmol), and the mixture was left overnight at room temperature to give a crude product. After the solvent was removed with a stream of nitrogen gas, the residue was spotted on a preparative silica gel TLC plate (*n*-hexane:2-propanol = 96:4) and comigrated with an authentic sample of nonradioactive TDF. The silica gel corresponding to the nonradioactive TDF, $R_f = 0.20$, was removed, and the product was extracted with CH_2Cl_2, which resulted in a specific activity of 11.9 Ci/mmol. The structure of nonradioactive TDF was characterized by ^{1}H NMR and MS spectra. The values were as follows: ^{1}H NMR (300 MHz, $CDCl_3$) δ 2.33 (s, 3H), 3.59 (s, 3H), 5.03 (s, 2H), 5.36 (s, 2H), 6.86 (d, $J = 8.1$ Hz, 2H), 7.08 (m, 1H), 7.21 (d, $J = 8.1$ Hz, 2H), 7.25−7.35 (m, 4H), 7.46 (d, $J = 8.2$ Hz, 2H), 7.82 (s, 1H), 7.98 (d, $J = 8.2$ Hz, 2H); ESI-MS (*m*/*z*) 564 $[M + H]^+$.

Enzyme Activity. The standard assay mixture contained 0.25 M sucrose, 50 mM sodium phosphate (pH 7.5), 1 mM EDTA, and SMP (10−30 μg/mL). Activities were assayed at 30 °C as a decrease of absorbance at 340 nm with

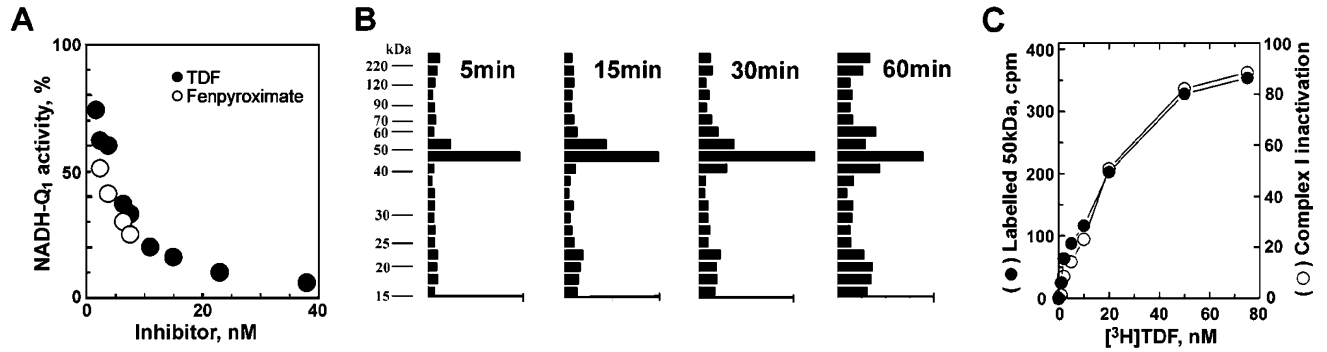

FIGURE 3: Inhibition and labeling of bovine SMP with TDF. (A) Concentration-dependent inhibition of NADH−UQ1 reductase activity in bovine SMP by TDF and fenpyroximate. (B) Time dependence of photoaffinity labeling of the 50 kDa band with [^{3}H]TDF pretreated with NADH (400 μM). A 13.5% gel was used. Each calibration bar at the bottom designates 10^3 cpm/ sample (2.7×10^4 cpm/mg of protein). (C) Correlation between the incorporation of radioactivity into the 50 kDa band and inhibition of the NADH oxidase activity. SMP were UV-illuminated for 5 min with [^{3}H]TDF at the concentrations indicated without NADH activation. See Materials and Methods for details.

150 μM NADH (NADH oxidase) or with 150 μM NADH and 100 μM UQ1 in the presence of 2 mM KCN and 0.2 μM antimycin A (NADH−UQ1 reductase). The NADH−$K_3Fe(CN)_6$ reductase was determined from an absorbance decrease at 420 nm with 150 μM NADH and 1 mM $K_3Fe(CN)_6$.

Photoaffinity Labeling. SMP (0.2 mg/mL) in a buffer containing 250 mM sucrose and 50 mM sodium phosphate (pH 7.5) were treated with [^{3}H]TDF (typically 20 nM) for 10 min at room temperature, then 400 μM NAD(P)H plus 1 mM sodium pyruvate was added for activation (*30*), and the incubation was continued for 10 min. Residual NADH (NADPH) was oxidized by L-lactate dehydrogenase (type II, from rabbit muscles) before photoirradiation to prevent quenching of the UV light (*27*). Samples were then irradiated for 5−20 min at 4 °C under a 12 W UV lamp (365 nm) at a distance of 2−3 cm. The SMP were pelleted (15 min, 50000 rpm, 4 °C) and subjected to various gel electrophoresis analyses. The gels were cut into 1−2.5 mm slices and individually digested overnight with 0.5−0.75 mL of 30% H_2O_2 at 75 °C, then mixed with 5−10 mL of Beta Blend scintillation mixture, and counted for ^{3}H radioactivity in a Beckman LS-1801 scintillation counter. Inhibitors (in ethanol) were added to SMP suspensions on ice for 10 min prior to incubation with [^{3}H]TDF. Final concentrations of ethanol in SMP suspensions were less than 1%.

Electrophoresis. SDS−PAGE was performed according to Laemmli (*31*) or Schagger and Von Jagow (*32*). For the separation of complex I from SMP, BN-PAGE was carried out on a 5−12% linear acrylamide gradient using a full-sized gel format (*33*). The complex I band was confirmed by activity staining using NADH and nitroblue tetrazolium (*34*). The 2-DE was performed by the method of O'Farrel (*35*) with some modifications. IEF gels were made in glass tubing (180 × 2.5 mm) by loading the gel mixture: 9 M urea; 4%/0.2% acrylamide/bisacrylamide; 2% Triton X-100; 2% ampholine (pH 3.5−10, Amarsham Pharmacia Biotech) with ammonium persulfate/*N*,*N*,*N*′,*N*′-tetramethylethylenediamine. We used fully degassed 1 M NaOH and 10 mM phosphoric acid for cathode and anode buffers, respectively. First dimension: SMP (4 mg/mL) was solubilized in the sample buffer containing 8 M urea, 4% CHAPS, 50−100 mM dithiothreitol, 40 mM Tris (*36*), and 0−6% SDS. After the samples (10−25 μL) were loaded, the gels were run for 15−24 h at 200 V because protein bands close to cathode became severely distorted when IEF was done at >200 V. Second dimension: IEF gels were equilibrated with SDS gel sample buffer for 3−4 h at room temperature and placed on top of tricine slab gels (16.5% T/3% C). Gels were run in duplicates. One set was stained with CBB and used for radioactivity counting. The other was, for immunoblot analyses, transferred onto 0.2 μm nitrocellulose membranes using the standard procedure (*37*) or PVDF membranes for 15−20 h at 35 V (or 250 mA) in a buffer containing 10 mM Na_2CO_3, 3 mM $NaHCO_3$, and 0.025% SDS according to ref *38*. To check the pH gradient in IEF patterns, the IEF disk gels were cut into 5 mm sections which were placed in individual tubes with 2 mL of freshly prepared degassed H_2O. These vials were capped and shaken for 30 min, and then the pH was measured on a pH meter. We compared the obtained pH curve with the IEF standard pattern (Bio-Rad, ranging from 4.45 to 9.6).

Immunochemical Analyses. We attempted to raise antibody to the C-terminal region of the bovine ND5 subunit using a nanopeptide, Cys-Ser-Met-Ile-Leu-Phe-Asn-Phe-His-Glu, conjugated to maleimide-activated BSA. Unfortunately, antibody thus produced only weakly recognized the ND5 subunit. Immunoblotting was conducted as described previously (*37*, *39*). The final detection was performed with enhanced chemiluminescence, Supersignal kits (Pierce, Rockford, IL). Immunoprecipitation was performed according to the literature (*20*, *40*).

Other Analytical Procedures. Protein concentrations were estimated by the method of Lowry et al. (*41*) with BSA as the standard. Any variations from the procedures and other details are described in the figure legends.

RESULTS

Photoaffinity Labeling of SMP. Figure 3A reveals effects of fenpyroximate and its photoreactive analogue, TDF, on the NADH−UQ1 reductase activity of bovine heart SMP. Despite considerable gain in bulkiness as compared to fenpyroximate, TDF retained inhibitor potency (I_{50} = ∼5 nM) remarkably well. Like fenpyroximate, inhibition by TDF was specific for complex I with no appreciable effects on other segments of the respiratory chain. UV irradiation of SMP in the presence of a low concentration (20 nM) of [^{3}H]-TDF resulted in one solely labeled region with an apparent M_r of ∼50 kDa on a SDS gel. Nearly 90% of labeling

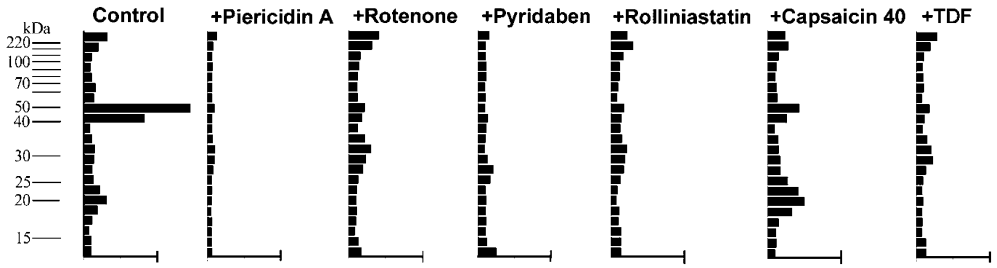

FIGURE 4: Effects of various complex I inhibitors on [^{3}H]TDF labeling of the 50 kDa band. Bovine heart SMP were treated with each inhibitor (2 μM) for 10 min on ice and incubated with [^{3}H]TDF (20 nM) for 10 min at room temperature. Then, the SMP suspension was incubated with NADH (400 μM) for 10 min at room temperature. After the remaining NADH was oxidized by L-lactate dehydrogenase, the suspension was illuminated under UV for 20 min at 4 °C as described in Materials and Methods.

Table 1: Effects of Nucleotides on the Labeling of the 50 kDa Band by [^{3}H]TDF

additions	relative amount of radioactivity incorporated (%)
control	100[a]
NADH (4 μM)	149
NADH (40 μM)	185
NADH (400 μM)	246
NADPH (4 μM)	157
NADPH (40 μM)	204
NADPH (400 μM)	248
NAD (400 μM)	~100
NADP (400 μM)	~100
ATP (400 μM)	~100

[a] 100% indicated 19500 cpm/mg of SMP.

completed within 5 min of photoactivation (Figure 3B). Longer illumination (>30 min) caused higher background owing to nonspecific binding (Figure 3B). Similar high background was observed when SMP were treated with 100 nM [^{3}H]TDF or at 1 mg/mL SMP suspension (data not shown). As shown in Figure 3C, a good correlation was found between the incorporation of radioactivity into the 50 kDa band and inhibition of the NADH oxidase activity. It is conceivable that the photolabeled 50 kDa protein is responsible for the inactivation of complex I. The maximum amount of [^{3}H]TDF bound to SMP was estimated to be ~0.1 nmol/mg of SMP at a TDF concentration of 20 nM.

Effects of Cofactors. NADH has been reported to increase the photoaffinity labeling of inhibitor/quinone probes in complex I when SMP was used (*18*, *27*). It was speculated that the bound UQ10 dissociates from complex I in the reduced state, resulting in an increase in accessibility of the inhibitor/quinone-binding site. Table 1 displays effects of various cofactors on the [^{3}H]TDF labeling. NAD, NADP, or ATP had essentially no effect. In contrast, NADH and NADPH significantly enhanced the labeling in a concentration-dependent manner, and the extent of enhancement was similar up to a concentration of 400 μM. It seems unlikely that the observed effects of NADH and NADPH are related to the enzyme catalytic activity of complex I because K_m values are vastly different between NADH (5−7 μM) and NADPH (550 μM) (*42*, *43*). Moreover, in a similar experiment with a [^{3}H]pyridaben analogue, the *P. denitrificans* Nqo6 (PSST) subunit was not influenced by prior NADH incubation (Dr. T. Yano, personal communication). It is known that the bovine complex I contains NADH/NADPH binding subunits (42, 39, and 30 kDa) in addition to the catalytic FP 51 kDa subunit (*44*). These subunits might be involved in the enhancement of labeling by NADH/NADPH.

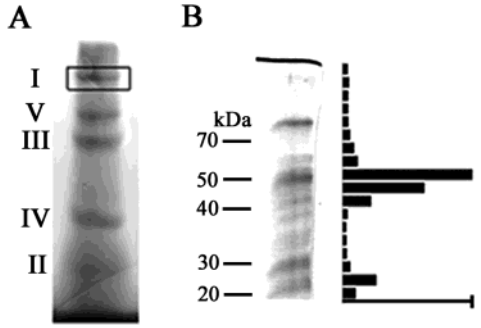

FIGURE 5: Localization of the labeled 50 kDa band in SMP. (A) Separation of the five oxidative phosphorylation enzyme complexes from [^{3}H]SMP (500 μg) by BN-PAGE (a 5−13% gradient gel). (B) SDS−PAGE analysis of complex I isolated from (A) on a 12.5% gel. The calibration bar at the bottom designates 3×10^3 cpm/ sample (6×10^4 cpm/mg of protein).

Labeling Protection by Various Complex I Inhibitors. We compared the effects of various complex I inhibitors on the labeling with [^{3}H]TDF in Figure 4. As shown in Figure 1, the structures of these inhibitors are significantly diverse. The labeling of the 50 kDa band was blocked by piericidin A, rotenone, pyridaben, rolliniastatin I, capsaicin 40, and nonradiolabeled TDF at 2 μM, at which each compound fully inhibited NADH oxidase activity (*45*). These results may suggest that [^{3}H]TDF shares a common binding site with other complex I inhibitors. Similar trends were reported with [^{3}H]pyridaben analogue labeling of the PSST subunit (*27*).

Identification of the Photoaffinity-Labeled 50 kDa Protein in Bovine SMP. [^{3}H]TDF-labeled SMP were subjected to BN-PAGE and resolved into five enzyme complexes (Figure 5A). Distribution of radioactivity among the complexes was determined to be complexes I (86%), II (4.3%), III (2.7%), IV (3.8%), and V (4.1%). Clearly, radiolabeling occurred predominantly in complex I. The labeled complex I was subjected to the SDS−PAGE for further separation. As shown in Figure 5B, we detected a major radioactivity peak at around 50 kDa and a small peak at around 23 kDa. The 23 kDa band was confirmed to be the PSST subunit by immunoprecipitation (data not shown). Among the subunits of bovine complex I, those that migrate at approximately 50 kDa include the FP 51 kDa, the IP 49 kDa, and the ND5 (the predicted molecular mass is 66 kDa but the apparent M_r is 45−50 kDa on SDS gels) subunit.

It is known that the peripheral subunits can be extracted from the membranes by chaotropes or alkaline pH (*46*, *47*). When the bovine SMP labeled by [^{3}H]TDF were treated with a chaotrope (8 M urea, 2 M NaI, or 0.5 M $NaClO_4$), or alkaline pH (pH 12), most of the radioactivity remained in

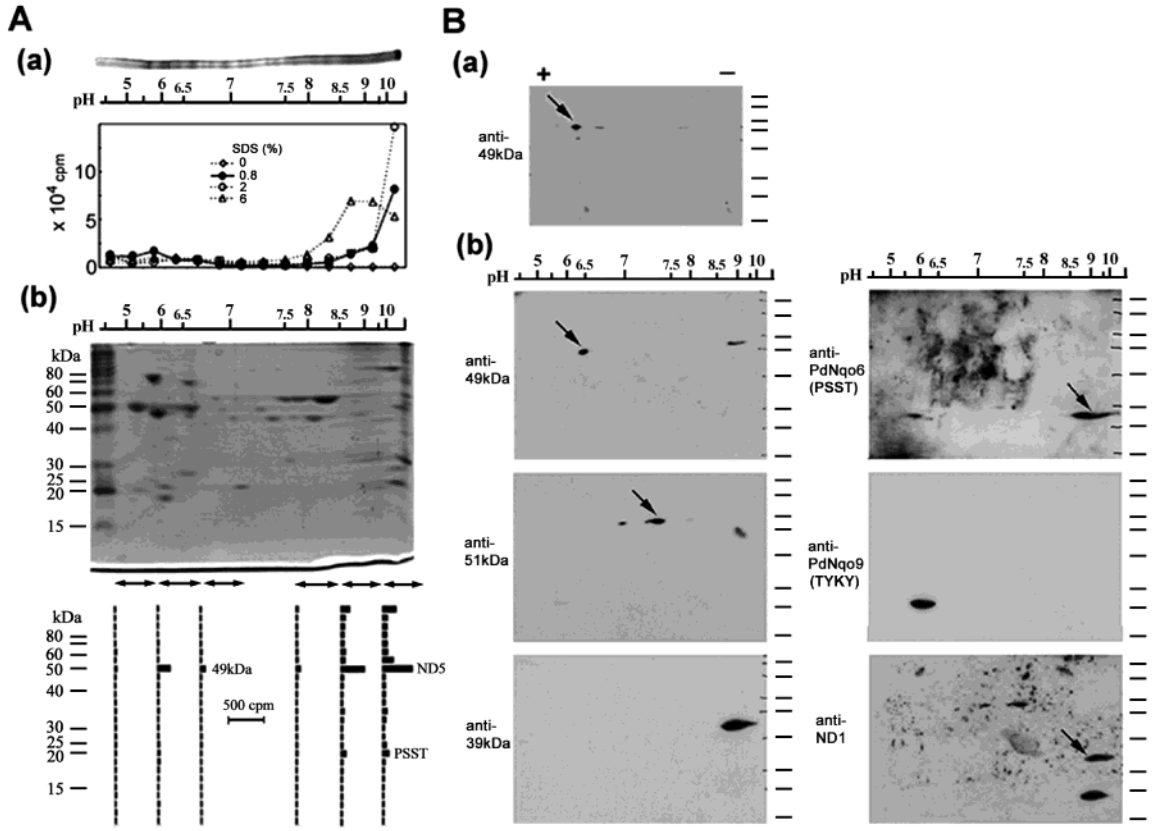

FIGURE 6: Identification of the photoaffinity-labeled 50 kDa protein in complex I by 2-D gel analyses (IEF and SDS−PAGE). (A) (a) A CBB-stained, one-dimensional IEF gel pattern of [^{3}H]SMP solubilized in IEF sample solution containing 0.8% SDS and the effect of SDS on the recovery of radioactivity in IEF gels. (b) 2-D separation of [^{3}H]SMP solubilized in the presence of 0.8% SDS (on a Schagger's 16.5% C/3% T gel) and localization of radioactivity by SDS−PAGE analyses in the marked areas. (B) (a) Identification of the IP 49 kDa spot on a 2-DE gel (6% SDS was used for solubilization) by western blotting with anti-IP 49 kDa antiserum. (b) Immunoblotting analyses of 2-D gels prepared as in Figure 5A and transferred to a PVDF membrane by using anti-IP 49 kDa, anti-51 kDa, anti-ND1, anti-*Pd*Nqo6 (for PSST detection), and anti-*Pd*Nqo9 (for TYKY) antisera and anti-mouse 39 kDa monoclonal antibody. The bars at the right side of each panel indicate the molecular markers (from the top to the bottom: 114, 81, 64, 50, 37, 26, 20, and 15 kDa). Predicted molecular mass and p*I* values of the individual subunits are IP 49 kDa (49174/6.33), FP 51 kDa (48499/7.32), TYKY (23896/6.84), 39 kDa (42848/10.39), PSST (20077/10.53), ND1 (35669/8.42), and ND5 (68277/10.01).

the membranes (data not shown). Furthermore, the labeled protein resisted chloroform/methanol extraction. These properties of the labeled 50 kDa protein suggest that it is in the membrane domain, which would exclude the 51 and the 49 kDa subunits.

To identify the radiolabeled protein more explicitly, we carried out 2-DE analysis that would offer better separation of the three candidate subunits because of vast differences in the predicted p*I* values: IP 49 kDa (6.33), FP 51 kDa (7.32), and ND5 (10.02). It is known that highly hydrophobic membrane proteins are hardly detected on 2-DE gels, and loading 2-DE gels with large amounts of membrane proteins results in a severe loss of hydrophobic proteins due to precipitation at their p*I* values, and there are difficulties in the separation in the alkali range (*48*, *49*). However, as shown in Figure 6A (a), the entry of radioactivity into IEF gels was clearly improved by elevating the SDS concentration to 2% or higher. Figure 6A (b) illustrates that most of radioactivity associated with the 50 kDa protein mainly appeared at pI = 9−10 and less at pI = 6−6.5. It is, therefore, conceivable that the labeled 50 kDa protein exhibiting pI = 9−10 is the ND5 subunit. It should also be noted that the 50 kDa band is not discernible in CBB staining under the conditions employed, which agrees with the fact that the ND5 protein is difficult to stain. The pI = 6−6.5 band was recognized by the anti 49 kDa subunit antibody. Table 2 shows total radioactivity of the 50 kDa protein recovered from the two regions (pI = 6−6.5 and 9−10) of 2-DE gels with increasing concentrations of SDS (used for solubilization). Radioactivity at pI = 9−10 (predominantly the ND5 subunit) increased as the concentration of SDS was raised, suggesting that higher concentrations of SDS allowed more protein to enter the gel. In contrast, the 50 kDa protein at pI = 6−6.5 (49 kDa subunit) migrated similarly, regardless of the SDS concentration. In addition, we detected a very small but significant amount of radioactivity in the PSST spot, which was already recognized in Figure 5B. The radioactivity of PSST was increased to 814 cpm at 6% SDS from 216 cpm at 0.8%. In Figure 6B, gels run under conditions identical

Table 2: Effect of SDS on Extraction of [^{3}H]TDF-Labeled Subunits from Bovine Heart SMP[a]

	50 kDa (×10^2 cpm)	
SDS (%)	pI = 6−6.5	pI = 9−10
0	3.3	1.1
0.8	4.4	11.5
2.0	4.8	15.2
6.0	4.3	48.9

[a] Bovine heart SMP (100 μg) labeled by [^{3}H]TDF were incubated with various concentrations of SDS and then subjected to the 2-DE analyses.

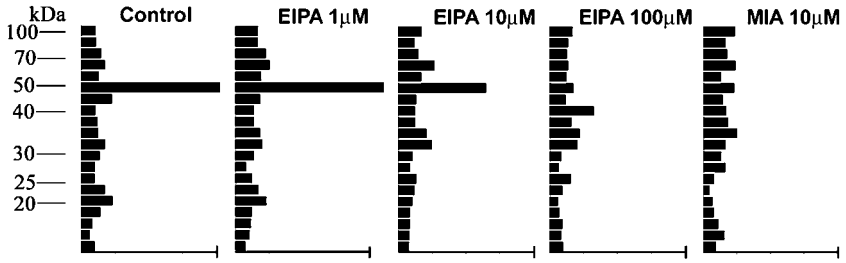

FIGURE 7: Effects of amiloride derivatives EIPA and MIA on [^{3}H]TDF labeling of the 50 kDa band. Each calibration bar at the bottom designates 10^3 cpm/sample (2.7×10^4 cpm/mg of protein).

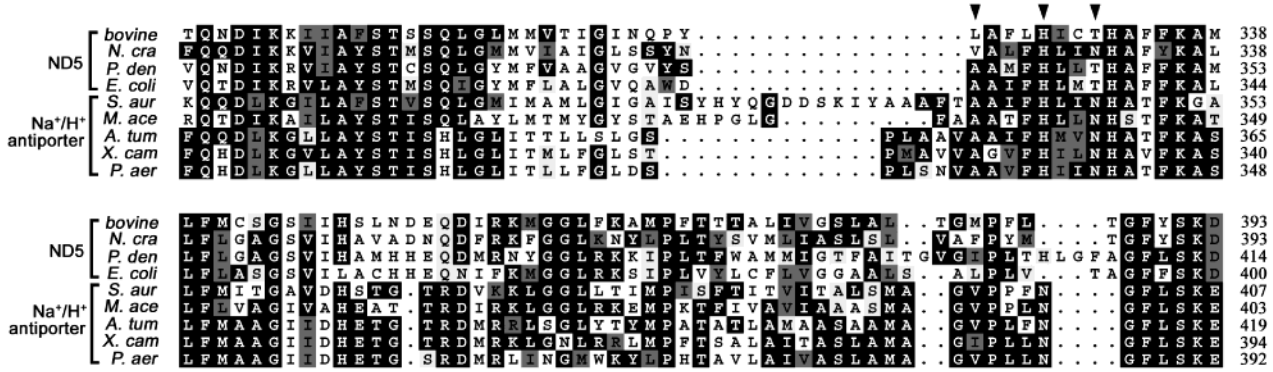

FIGURE 8: Comparison of the deduced primary sequences between the predicted Q-binding domain of ND5 subunits and MnhA subunits of the Na^+/H^+ antiporter complex encoded by the *Mnh* operons. The sequences from *Bos taurus* ND5 (bovine; accession number P03920), *Neurospora crassa* ND5 (*N. cra*; S10843), *Paracoccus denitirificans* Nqo12 (*P. den*; NQOC_PARDE), *Escherichia coli* NuoL (*E. coli*; NP_416781), *Staphylococcus aureus* MnhA (*S. aur*; NP_645651), *Methanosarcina acetivorans* MnhA (*M. ace*; NP_619431), *Agrobacterium tumefaciens* MnhA (*A. tum*; NP_531214), *Xanthomonas campestris* MnhA (*X. cam*; NP_635840), and *Pseudomonas aeruginosa* MnhA (*P. aer*; NP_249745) were aligned by using the program PILEUP of the Wisconsin Package, Accelrys Inc. (San Diego, CA). Conserved residues are highlighted by black boxes (identical) and shadowed boxes (similar). A possible Q-binding motif (L/A-X_3-H-X_2-T) in complex I predicted by Fisher and Rich (*75*) is shown by arrowheads. In the case of the *N. crassa* ND5 subunit, the first and the third amino acids of the triad are replaced by V and N, respectively. It seems interesting that the sequences in this domain of MnhA subunits from various organisms are well conserved (A-X_3-H-X_2-N) and similar to those of the ND5 subunits.

to Figure 6A (b) were analyzed by immunoblotting to localize each individual complex I subunit on a PVDF. All of the subunits examined here basically migrated according to the anticipated p*I* and their molecular size as previously reported (*50*). Although spots in the alkaline region tended to diffuse due to SDS, the separation patterns remained the same when compared to those in the absence of SDS. For instance, TYKY (pI = 6.84) migrated to a little more acidic region than 49 kDa (pI = 6.33) [Figure 6B (b)] as previously shown in refs *51* and *52*. Our data demonstrated that IEF can be carried out in the presence of SDS at as high as 0.8% or even at 6% if limited in the neutral to acidic region [Figure 6B(a)]. For complete dissociation of the IP 49 kDa subunit from the enzyme complex, 2% or higher SDS was needed [Figure 6B(a)].

Effect of Na^+/H^+ Antiporter Inhibitors on the Labeling. Recent literature reported that the ND5 subunit exhibits sequence similarity to the MnhA subunit of the Na^+/H^+ antiporter of *Staphylococcus aureus* which is composed of seven different subunits (designated MnhA−G) (*53*−*55*). In fact, it was shown by Steuber et al. that *E. coli* and *Klebsiella pneumoniae* NDH-1 could function as the Na^+ pump (*56*). We studied effects of two specific inhibitors for Na^+/H^+ transporters on the photolabeling. As shown in Figure 7, EIPA, an amiloride derivative inhibitor (see Figure 1C for the chemical structure), suppressed the labeling of the ND5 subunit with [^{3}H]TDF in a dose-dependent manner. Another amiloride derivative inhibitor, MIA, completely prevented the labeling at 10 μM. It is speculated that amilorides inhibit single subunit Na^+/H^+ antiporters by binding to the Na^+ site (*57*, *58*). It is not known whether multisubunit Na^+/H^+ antiporters encoded by the *Mnh* operons are also inhibited by amilorides. Therefore, we examined effects of the two inhibitors on the NADH oxidase and NADH−UQ1 and NADH−$K_3Fe(CN)_6$ reductase activities of bovine SMP. It turned out that both compounds inhibited the NADH oxidase of bovine SMP. The inhibition by EIPA was 2.7%, 57.7%, and 98.9% at 1 μM, 10 μM, and 100 μM, respectively, and the inhibition by MIA was 95% at 10 μM. Similar inhibition was observed with the NADH−UQ1 reductase activity. In contrast, neither EIPA or MIA affected NADH−$K_3Fe(CN)_6$ reductase activity of SMP. Thus, labeling protection by EIPA and MIA seems to be correlated with their inhibitory effects of energy-coupled complex I activity. As far as our present knowledge is concerned, this is a first report that amiloride derivatives act as inhibitors of energy-coupled activities of bovine heart complex I.

DISCUSSION

Data available to date indicate that the inhibitor/Q-binding pocket in complex I spans the subunits IP 49 kDa, PSST, ND1, and ND3. On the basis of deduced primary sequence analyses of ND5 and its homologues, the ND5 subunit has been predicted to participate in site 1 coupling and to house a Q-binding site but without any experimental results (see Figure 8). Our present study showed that the photoaffinity probe [^{3}H]TDF predominantly labeled the ND5 subunit. The labeling was displaced by various complex I inhibitors. The

data indicate that the ND5 subunit participates in making the inhibitor/Q-binding pocket. Taking into consideration that IP 49 kDa and PSST subunits were also labeled by [^{3}H]-TDF albeit partially, we speculate that the ND5 subunit may be close to the PSST and IP 49 kDa subunits. This seems to be in disagreement with the location of ND5 deduced from structural models of complex I based on low-resolution EM analyses (*38*, *59*). It is possible that some segment of the ND5 subunit is localized close to PSST and IP 49 kDa subunits, but this part is not recognized by low-resolution EM analyses of complex I. Another possibility is that NADH/NADPH induces a dynamic conformation change in complex I which alters relative positioning of certain subunits (*60*−*63*).

Steuber's group (*64*, *65*) demonstrated that the NDH-1 in *E. coli* and *K. pneumoniae* pumps not only H^+ but also Na^+. They hypothesized that the bacterial ND5 (Nqo12/NuoL) homologues may contribute to H^+/Na^+ pump activity in NDH-1 based on high sequence similarity between the ND5 subunit and Na^+/H^+ antiporters (see Figure 8). Interestingly, amilorides that are known to be inhibitors of Na^+/H^+ antiporters also inhibited the complex I activity of bovine heart SMP in the physiological concentration range. In addition, they suppressed the labeling of the 50 and 23 kDa bands by [^{3}H]TDF. A question arises as to where the amiloride-binding site is located in the ND5 subunit. Tsuchiya's group reported that the sequence $V^{62}FF^{64}$ (*Vibrio parahaemolyticus* numbering) is highly conserved among the single-subunit Na^+/H^+ antiporter NhaA, the Na^+/H^+ exchangers in mammalian cells, and the *E. coli* melibiose transporter (a Na^+-coupled symporter) (*66*). They carried out mutation experiments of *V. parahaemolyticus* NhaA (V62L, F63Y, and F64Y) (*66*). The amiloride-binding affinity decreased 10-fold with the mutant F64Y and 2-fold with the mutant F63Y but was almost unchanged with the mutant V62L. Together, they hypothesized that the VFF sequence is one of the motifs involved in Na^+ binding and amiloride binding. We searched for the VFF motif in the bovine ND5 subunit sequence. While there is no VFF motif, the bovine ND5 subunit harbors three FF motifs ($K^{116}FF$, $A^{333}FF$, and $I^{427}FF$). Of these three, $A^{333}FF$ is highly conserved among the ND5 subunit and its homologues in various organisms, although in the *N. crassa* ND5 subunit AFF is replaced by AFY (Figure 8). It is interesting that $A^{333}FF$ is located immediately downstream of the predicted Q-binding site (L/A-X_3-H-X_2-T). Piericidin A and capsaicin 40, which are considered to be structurally similar to Q, also diminished [^{3}H]TDF labeling. Together, the data in this study may support the hypothesis that the ND5 subunit plays key roles in inhibitor/Q-binding and H^+/Na^+ translocation in complex I/NDH-1. The physiological importance of the ND5 subunit is apparent from other observations that complex I-dependent respiration is tightly regulated by ND5 gene expression (*67*) and that the ND5 subunit is essential for the activity of complex I (*68*, *69*). Our knowledge on the membrane domain subunits in complex I/NDH-1 is considerably limited despite some recent studies (*25*, *70*−*74*). Thorough studies on the membrane domain including the ND5 subunit are prerequisites to understand the underlying mechanism of electron transfer and energy coupling of complex I at the molecular level.

ACKNOWLEDGMENT

We thank Drs. C.-A. Yu, Y. Hatefi, S. Yoshida, and E. Estornell for kindly providing us with their valuable materials. We are grateful to Drs. Salvatore Di Bernardo, Byoung Boo Seo, Mou-Chieh Kao, and Isabel Velázquez for helpful advice and stimulating discussion.

REFERENCES

1. Scheffler, I. E. (1999) *Mitochondria*, Wiley-Liss, New York.
2. Saraste, M. (1999) Oxidative phosphorylation at the *fin de siècle*, *Science 283*, 1488−1493.
3. Walker, J. E. (1992) The NADH:ubiquinone oxidoreductase (complex I) of respiratory chains, *Q. Rev. Biophys. 25*, 253−324.
4. Fearnley, I. M., Carroll, J., Shannon, R. J., Runswick, M. J., Walker, J. E., and Hirst, J. (2001) GRIM-19, a cell death regulatory gene product, is a subunit of bovine mitochondrial NADH: ubiquinone oxidoreductase (complex I), *J. Biol. Chem. 276*, 38345−38348.
5. Chomyn, A., Mariottini, P., Cleeter, M. W. J., Ragan, C. I., Matsuno-Yagi, A., Hatefi, Y., Doolittle, R. F., and Attardi, G. (1985) Six Unidentified Reading Frames of Human Mitochondrial DNA Encode Components of the Respiratory-Chain NADH Dehydrogenase, *Nature 314*, 591−597.
6. Chomyn, A., Cleeter, M. W. J., Ragan, C. I., Riley, M., Doolittle, R. F., and Attardi, G. (1986) URF6, last unidentified reading frame of human mtDNA, codes for an NADH dehydrogenase subunit, *Science 234*, 614−618.
7. Fearnley, I. M., and Walker, J. E. (1992) Conservation of sequences of subunits of mitochondrial complex I and their relationships with other proteins, *Biochim. Biophys. Acta 1140*, 105−134.
8. Wallace, D. C. (1999) Mitochondrial diseases in man and mouse, *Science 283*, 1482−1488.
9. Jenner, P. (2001) Parkinson's disease, pesticides and mitochondrial dysfunction, *Trends Neurosci. 24*, 245−246.
10. Matsuno-Yagi, A., and Yagi, T., Eds. (2001) Complex I, *J. Bioenerg. Biomembr. 33*, 155−266.
11. Miyoshi, H. (1998) Structure−activity relationships of some complex I inhibitors, *Biochim. Biophys. Acta 1364*, 236−244.
12. Miyoshi, H. (2001) Probing the ubiquinone reduction site in bovine mitochondrial complex I using a series of synthetic ubiquinones and inhibitors, *J. Bioenerg. Biomembr. 33*, 223−231.
13. Earley, F. G., and Ragan, C. I. (1984) Photoaffinity labelling of mitochondrial NADH dehydrogenase with arylazidoamorphigenin, an analogue of rotenone, *Biochem. J. 224*, 525−534.
14. Earley, F. G. P., Patel, S. D., Ragan, C. I., and Attardi, G. (1987) Photolabelling of a mitochondrially encoded subunit of NADH dehydrogenase with [^{3}H]dihydrorotenone, *FEBS Lett. 219*, 108−113.
15. Yagi, T. (1987) Inhibition of NADH-ubiquinone reductase activity by *N*′,*N*′-dicyclohexylcabodiimide and correlation of this inhibition with the occurrence of energy coupling site 1 in various organisms, *Biochemistry 26*, 2822−2828.
16. Yagi, T., and Hatefi, Y. (1988) Identification of the DCCD-Binding Subunit of NADH−Ubiquinone Oxidoreductase (Complex I), *J. Biol. Chem. 263*, 16150−16155.
17. Hassinen, I. E., and Vuokila, P. T. (1993) Reaction of dicyclohexylcarbodiimide with mitochondrial proteins, *Biochim. Biophys. Acta 1144*, 107−124.
18. Heinrich, H., and Werner, S. (1992) Identification of the ubiquinone-binding site of NADH:ubiquinone oxidoreductase (complex I) from *Neurospora crassa*, *Biochemistry 31*, 11413−11419.
19. Heinrich, H., Azevedo, J. E., and Werner, S. (1992) Characterization of the 9.5-kDa ubiquinone-binding protein of NADH: ubiquinone oxidoreductase (complex I) from *Neurospora crassa*, *Biochemistry 31*, 11420−11424.
20. Schuler, F., Yano, T., Di Bernardo, S., Yagi, T., Yankovskaya, V., Singer, T. P., and Casida, J. E. (1999) NADH-quinone oxidoreductase: PSST subunit couples electron transfer from iron−sulfur cluster N2 to quinone, *Proc. Natl. Acad. Sci. U.S.A. 96*, 4149−4153.
21. Ohnishi, T. (1998) Iron−sulfur clusters semiquinones in Complex I, *Biochim. Biophys. Acta 1364*, 186−206.
22. Darrouzet, E., Issartel, J. P., Lunardi, J., and Dupuis, A. (1998) The 49-kDa subunit of NADH-ubiquinone oxidoreductase (Com-

plex I) is involved in the binding of piericidin and rotenone, two quinone-related inhibitors, *FEBS Lett. 431*, 34−38.
23. Dupuis, A., Prieur, I., and Lunardi, J. (2001) Toward a characterization of the connecting module of complex I, *J. Bioenerg. Biomembr. 33*, 159−168.
24. Kashani-Poor, N., Zwicker, K., Kerscher, S., and Brandt, U. (2001) A central functional role for the 49 kDa subunit within the catalytic core of mitochondrial complex I, *J. Biol. Chem. 276*, 24082−24087.
25. Di Bernardo, S., and Yagi, T. (2001) Direct interaction between a membrane domain subunit and a connector subunit in the H^+-translocating NADH-quinone oxidoreductase, *FEBS Lett. 508*, 385−26.
26. Yagi, T., Di Bernardo, S., Nakamaru-Ogiso, E., Kao, M.-C., Seo, B. B., and Matsuno-Yagi, A. (2003) in *Respiration in Archaea and Bacteria* (Zannoni, D., Ed.) Kluwer Publishings, Dordrecht (in press).
27. Schuler, F., and Casida, J. E. (2001) Functional coupling of PSST and ND1 subunits in NADH:ubiquinone oxidoreductase established by photoaffinity labeling, *Biochim. Biophys. Acta 1506*, 79−87.
28. Matsuno-Yagi, A., and Hatefi, Y. (1985) Studies on the Mechanism of Oxidative Phosphorylation: Catalytic Site Cooperativity in ATP Synthesis, *J. Biol. Chem. 260*, 14424−14427.
29. Resek, J. F., Bhattacharya, S. K., and Khorana, H. G. (1993) A new photo-crosslinking reagent for the study of protein−protein interactions, *J. Org. Chem. 58*, 7598−7601.
30. Galkin, A. S., Grivennikova, V. G., and Vinogradov, A. D. (1999) $\rightarrow H^+/2(e)$ stoichiometry in NADH-quinone reductase reactions catalyzed by bovine heart submitochondrial particles, *FEBS Lett. 451*, 157−161.
31. Laemmli, U. K. (1970) *Nature 227*, 680−685.
32. Schagger, H., and Von Jagow, G. (1987) Tricine-sodium dodecyl sulfate-polyacrylamide gel electrophoresis for the separation of proteins in the range from 1 to 100kDa, *Anal. Biochem. 166*, 368−379.
33. Schagger, H. (1995) Native electrophoresis for isolation of mitochondrial oxidative phosphorylation protein complexes, *Methods Enzymol. 260*, 190−202.
34. Zerbetto, E., Vergani, L., and Dabbeni-Sala, F. (1997) Quantification of muscle mitochondrial oxidative phosphorylation enzymes *via* histochemical staining of blue native polyacrylamide gels, *Electrophoresis 18*, 2059−2064.
35. O'Farrell, P. H. (1975) High-resolution two-dimensional electrophoresis of proteins, *J. Biol. Chem. 250*, 4007−4021.
36. Herbert, B. (1999) Advances in protein solubilisation for two-dimensional electrophoresis, *Electrophoresis 20*, 660−663.
37. Hekman, C., Tomich, J. M., and Hatefi, Y. (1991) Mitochondrial ATP Synthase Complex: Membrane Topography and Stoichiometry of the F_o Subunits, *J. Biol. Chem. 266*, 13564−13571.
38. Sazanov, L. A., Peak-Chew, S. Y., Fearnley, I. M., and Walker, J. E. (2000) Resolution of the membrane domain of bovine complex I into subcomplexes: implications for the structural organization of the enzyme, *Biochemistry 39*, 7229−7235.
39. Seo, B. B., Matsuno-Yagi, A., and Yagi, T. (1999) Modulation of oxidative phosphorylation of human kidney 293 cells by transfection with the internal rotenone-insensitive NADH-quinone oxidoreductase (*NDI1*) gene of *Saccharomyces cerevisiae*, *Biochim. Biophys. Acta 1412*, 56−65.
40. Anderson, D. J., and Blobel, G. (1983) Immunoprecipitation of proteins from cell-free translation, *Methods Enzymol. 96*, 111−120.
41. Lowry, O. H., Rosebrough, N. J., Farr, A. L., and Randall, R. J. (1951) *J. Biol. Chem. 193*, 265−275.
42. Vinogradov, A. D. (1993) Kinetics, control, and mechanism of ubiquinone reduction by the mammalian respiratory chain-linked NADH-ubiquinone reductase, *J. Bioenerg. Biomembr. 25*, 367−375.
43. Hatefi, Y., and Hanstein, W. G. (1973) Interactions of Reduced and Oxidized Triphosphopyridine Nucleotides with the Electron Transport System of Bovine Heart Mitochondria, *Biochemistry 12*, 3515−3522.
44. Yamaguchi, M., Belogrudov, G. I., Matsuno-Yagi, A., and Hatefi, Y. (2000) The multiple nicotinamide nucleotide-binding subunits of bovine heart mitochondrial NADH:ubiquinone oxidoreductase (complex I), *Eur. J. Biochem. 267*, 329−336.
45. Degli Esposti, M. (1998) Inhibitors of NADH-ubiquinone reductase: an overview, *Biochim. Biophys. Acta 1364*, 222−235.
46. Takano, S., Yano, T., and Yagi, T. (1996) Structural studies of the proton-translocating NADH-quinone oxidoreductase (NDH-1) of *Paracoccus denitrificans*: Identity, property, and stoichiometry of the peripheral subunits, *Biochemistry 35*, 9120−9127.
47. Yano, T., and Yagi, T. (1999) H^+-translocating NADH-quinone-oxidoreductase (NDH-1) of *Paracoccus denitrificans*: Studies on topology and stoichiometry of the peripheral subunits, *J. Biol. Chem. 274*, 28606−28611.
48. Ames, G. F., and Nikaido, K. (1976) Two-dimensional gel electrophoresis of membrane proteins, *Biochemistry 15*, 616−623.
49. Molloy, M. P. (2000) Two-dimensional electrophoresis of membrane proteins using immobilized pH gradients, *Anal. Biochem. 280*, 1−10.
50. Finel, M., Skehel, J. M., Albracht, S. P. J., Fearnley, I. M., and Walker, J. E. (1992) Resolution of NADH:ubiquinone oxidoreductase from bovine heart mitochondria into two subcomplexes, one of which contains the redox centers of the enzyme, *Biochemistry 31*, 11425−11434.
51. Dupuis, A., Skehel, J. M., and Walker, J. E. (1991) A homologue of a nuclear-coded iron−sulfur protein subunit of bovine mitochondrial complex I is encoded in chloroplast genomes, *Biochemistry 30*, 2954−2960.
52. Skehel, J. M., Fearnley, I. M., and Walker, J. E. (1998) NADH: Ubiquinone oxidoreductase from bovine heart mitochondria: sequence of a novel 17.2-kDa subunit, *FEBS Lett. 438*, 301−305.
53. Hiramatsu, T., Kodama, K., Kuroda, T., Mizushima, T., and Tsuchiya, T. (1998) A putative multisubunit Na^+/H^+ antiporter from *Staphylococcus aureus*, *J. Bacteriol. 180*, 6642−6648.
54. Friedrich, T., and Weiss, H. (1997) Modular evolution of the respiratory NADH:ubiquinone oxidoreductase and the origin of its modules, *J. Theor. Biol. 187*, 529−540.
55. Steuber, J. (2001) Na^+ translocation by bacterial NADH:quinone oxidoreductases: an extension to the complex-I family of primary redox pumps, *Biochim. Biophys. Acta 1505*, 45−56.
56. Steuber, J., Schmid, C., Rufibach, M., and Dimroth, P. (2000) Na^+ translocation by complex I (NADH:quinone oxidoreductase) of *Escherichia coli*, *Mol. Microbiol. 35*, 428−434.
57. Young-Mog, K., Tachibana, Y., Shimamoto, T., Shimamoto, T., and Tsuchiya, T. (1997) Inhibition of melibiose transporter by amiloride in *Escherichia coli*, *Biochem. Biophys. Res. Commun. 233*, 147−149.
58. Putney, L. K., Denker, S. P., and Barber, D. L. (2002) The changing face of the Na^+/H^+ exchanger, NHE1: structure, regulation, and cellular actions, *Annu. Rev. Pharmacol. Toxicol. 42*, 527−552.
59. Sazanov, L. A., and Walker, J. E. (2000) Cryo-electron Crystallography of Two Sub-complexes of Bovine Complex I Reveals the Relationship between the Membrane and Peripheral Arms, *J. Mol. Biol. 302*, 455−464.
60. Yamaguchi, M., Belogrudov, G. I., and Hatefi, Y. (1998) Mitochondrial NADH-ubiquinone oxidoreductase (complex I)—Effects of substrates on the fragmentation of subunits by trypsin, *J. Biol. Chem. 273*, 8094−8098.
61. Belogrudov, G. I., and Hatefi, Y. (1994) Catalytic sector of complex I (NADH:ubiquinone oxidoreductase): Subunit stoichiometry and substrate-induced conformation changes, *Biochemistry 33*, 4571−4576.
62. Vinogradov, A. D., and Grivennikova, V. G. (2001) The mitochondrial Complex I: progress in understanding of catalytic properties, *IUBMB Life 52*, 129−134.
63. Bottcher, B., Scheide, D., Hesterberg, M., Nagel-Steger, L., and Friedrich, T. (2002) A Novel, Enzymatically active conformation of the *Escherichia coli* NADH:Ubiquinone oxidoreductase (complex I), *J. Biol. Chem. 277*, 17970−17977.
64. Steuber, J. (2001) The Na^+-translocating NADH:quinone oxidoreductase (NDH I) from *Klebsiella pneumoniae* and *Escherichia coli*: Implications for the mechanism of redox-driven cation translocation by complex I, *J. Bioenerg. Biomembr. 33*, 179−186.
65. Gemperli, A. C., Dimroth, P., and Steuber, J. (2002) The respiratory complex I (NDH I) from *Klebsiella pneumoniae*, a sodium pump, *J. Biol. Chem., 277*, 33811−33817.
66. Kuroda, T., Shimamoto, T., Mizushima, T., and Tsuchiya, T. (1997) Mutational analysis of amiloride sensitivity of the NhaA

Na^+/H^+ antiporter from *Vibrio parahaemolyticus*, *J. Bacteriol. 179*, 7600−7602.
67. Bai, Y., Shakeley, R. M., and Attardi, G. (2000) Tight control of respiration by NADH dehydrogenase ND5 subunit gene expression in mouse mitochondria, *Mol. Cell. Biol. 20*, 805−815.
68. Hofhaus, G., and Attardi, G. (1995) Efficient selection and characterization of mutants of a human cell line which are defective in mitochondrial DNA-encoded subunits of respiratory NADH dehydrogenase, *Mol. Cell. Biol. 15*, 964−974.
69. Cardol, P., Matagne, R. F., and Remacle, C. (2002) Impact of Mutations Affecting ND Mitochondria-encoded Subunits on the Activity and Assembly of Complex I in *Chlamydomonas*. Implication for the Structural Organization of the Enzyme, *J. Mol. Biol. 319*, 1211−1221.
70. Roth, R., and Hagerhall, C. (2001) Transmembrane orientation and topology of the NADH:quinone oxidoreductase putative quinone binding subunit NuoH, *Biochim. Biophys. Acta 1504*, 352−362.
71. Di Bernardo, S., Yano, T., and Yagi, T. (2000) Exploring the Membrane Domain of the Reduced Nicotinamide Adenine Dinucleotide-Quinone Oxidoreductase of *Paracoccus denitrificans*: Characterization of the NQO7 Subunit, *Biochemistry 39*, 9411−9418.
72. Kao, M.-C., Di Bernardo, S., Matsuno-Yagi, A., and Yagi, T. (2002) Characterization of the Membrane Domain Nqo11 Subunit of the Proton-Translocating NADH-Quinone Oxidoreductase of *Paracoccus denitrificans*, *Biochemistry 41*, 4377−4384.
73. Zickermann, V., Barquera, B., Wikström, M., and Finel, M. (1998) Analysis of the pathogenic human mitochondrial mutation ND1/3460, and mutations of strictly conserved residues in its vicinity, using the bacterium *Paracoccus denitrificans*, *Biochemistry 37*, 11792−11796.
74. Kurki, S., Zickermann, V., Kervinen, M., Hassinen, I., and Finel, M. (2000) Mutagenesis of Three Conserved Glu Residues in a Bacterial Homologue of the ND1 Subunit of Complex I Affects Ubiquinone Reduction Kinetics but Not Inhibition by Dicyclohexylcarbodiimide, *Biochemistry 39*, 13496−13502.
75. Fisher, N., and Rich, P. R. (2000) A motif for quinone binding sites in respiratory and photosynthetic systems, *J. Mol. Biol. 296*, 1153−1162.

BI0269660